Mancilla, F. d. L., Heit, B., Morales, J., Yuan, X., Stich, D., Molina-Aguilera, A., Azañon, J. M., Martín, R. (2018): A STEP fault in Central Betics, associated with lateral lithospheric tearing at the northern edge of the Gibraltar arc subduction system. - *Earth and Planetary Science Letters*, *486*, pp. 32—40.

DOI: http://doi.org/10.1016/j.epsl.2018.01.008

Earth and Planetary Science Letters 486 (2018) 32–40

Contents lists available at ScienceDirect

Earth and Planetary Science Letters

www.elsevier.com/locate/epsl

A STEP fault in Central Betics, associated with lateral lithospheric tearing at the northern edge of the Gibraltar arc subduction system

Flor de Lis Mancilla [a,b,*], Benjamin Heit [c], Jose Morales [a,b], Xiaohui Yuan [c], Daniel Stich [a,b], Antonio Molina-Aguilera [a,b], Jose Miguel Azañon [d], Rosa Martín [a]

[a] Instituto Andaluz de Geofisica, Universidad de Granada, Campus de Cartuja, 18071, Granada, Spain
[b] Departamento de Fisica Teorica y del Cosmos, Facultad de Ciencias, Universidad de Granada, Campus de Fuente Nueva, 18071, Granada, Spain
[c] Deutsches GeoForschungsZentrum, GFZ, Telegrafenberg, 14473, Potsdam, Germany
[d] Departamento de Geodinámica, Facultad de Ciencias, Universidad de Granada, Campus de Fuentenueva, 18071, Spain

ARTICLE INFO

Article history:
Received 1 July 2017
Received in revised form 5 December 2017
Accepted 10 January 2018
Available online 28 January 2018
Editor: R. Bendick

Keywords:
westernmost Mediterranean subduction system
central Betics
sharp Moho step
STEP fault
positive tectonic flower structure

ABSTRACT

We study the crustal and lithospheric mantle structure under central Betics in the westernmost Mediterranean region by migrating P-receiver functions along a dense seismic profile (~2 km interstation distance). The profile, North–South oriented, probes the crustal structure of different geological units, from the Alboran domain in the south with metamorphic rocks, through the External Zones with sedimentary rocks to the Variscan terrains of the Iberian Massif in the north. From north to south, the Moho depth increases from ~30 km to ~46 km underneath the Guadix basin, due to the underthrusting of the Iberian crust below the Alboran crust, and suddenly shallows to ~30 km underneath the Internal Zones with a step of 17 km. This sharp Moho step correlates well with a lithospheric step of ~40 km, where the thickness of the lithosphere changes abruptly from ~100 km in the north to ~50 km in the south. We interpret this sharp and prominent lithospheric step as the termination of the Iberian lithosphere caused by a near-vertical STEP (Subduction-Transform-Edge-Propagator) fault that continues towards the surface as a positive flower tectonic structure of crustal scale. This STEP fault is located at the northern edge of the narrow Westernmost Mediterranean subduction system facilitating the slab rollback motion towards the west. The sharp termination of the Iberian lithosphere occurs under the contact between the Alpujarride and the Nevado-Filabride complexes of the Alboran domain in an ENE-WSW right-lateral transpressive shear zone. The thickest crust and lithosphere do not correlate with the highest topography along the profile suggesting that this high topography is a combined effect of the positive flower structure, and the push up of the asthenosphere produced by the removal of the Iberian lithosphere.

1. Introduction

At edges of a subduction system, STEP faults (Subduction-Transform-Edge-Propagator, also called tear fault) occur and enable the continuation of subduction (Govers and Wortel, 2005). These faults are strike-slip transfer faults that produce tearing in the subducted plate lithosphere and propagate, approximately, perpendicular to the subduction strike (Nijholt and Govers, 2015). The slab tearing may result in sharp changes in lithospheric and crustal thickness across the STEP fault, strike-slip motion in the upper plate and vertical motion between the two blocks of the underthrusting plate at both sides of the STEP fault (Govers and Wortel, 2005; Baes et al., 2011). In addition, the juxtaposition of overriding plate and the continental part of the subducting plate causes an increase of the crustal thickness that contributes to the relatively sharp contrast in the Moho depth.

Observations of faults produced by slab tearing (STEP fault) have been found in subduction system worldwide (e.g. North Fiji Basin, Eastern Caribbean plate, Sulawesi Indonesia, see e.g. Govers and Wortel, 2005) and in the Mediterranean region in particular: e.g. in Northern Apennines (e.g. Agostinetti, 2015), in the southern Tyrrhenian subduction system (e.g. Bianchi et al., 2016) and in the Hellenic arc (e.g. Pearce et al., 2012). While STEP faults at the subducting slab have been studied largely in last years, deformation produce at the top of them in the overridden plate is still poorly understood. Some observations correlate the location of the STEP faults in the subducting plate with a wide shear zone in

* Corresponding author at: Instituto Andaluz de Geofisica, Universidad de Granada, Campus de Cartuja, 18071, Granada, Spain.
E-mail address: florlis@ugr.es (F.d.L. Mancilla).

https://doi.org/10.1016/j.epsl.2018.01.008

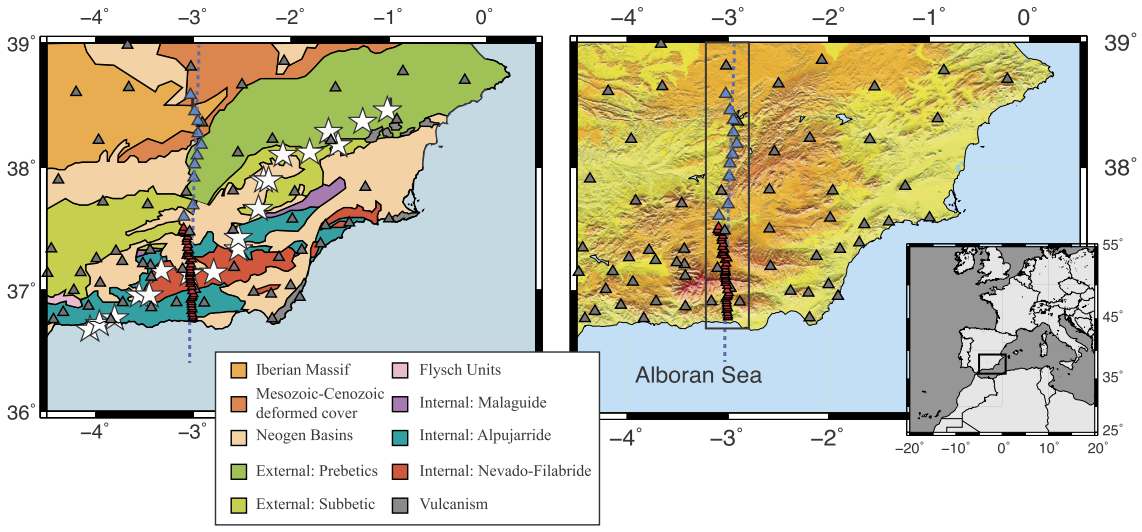

Fig. 1. Geologic (a) and topographic (b) maps. Red triangles mark the HIRE-I stations and black triangles the HIRE-II stations. Grey triangles denote the permanent and other previous temporary stations in the area. The white stars represent approximate location of the tear fault along the northern edges of the westernmost Mediterranean subduction system obtained by Mancilla et al. (2015a). The blue dashed line is the direction of the cross-sections shown in Figs. 2 and 4. The stations inside the black rectangle are the ones which data are included in the migration images.

the overriding plate formed by strike-slip faults (e.g. Özbakır et al., 2013; Agostinetti, 2015). Özbakır et al. (2013) following observations at the surface above the STEP fault suggested that the shear zone at depth is not sharp in its early stage of formation. However, there is no clear observation of how the deformation is distributed from the tear fault in the subducted slab to the entire crust in the overriding plate.

At the northern edge of the westernmost Mediterranean subduction system where continental crust started to be involved at Miocene ages, slab tearing along STEP fault has been suggested to occur (e.g. Faccenna et al., 2004; Duggen et al., 2004, 2005; Govers and Wortel, 2005; García-Castellanos and Villaseñor, 2011; Mancilla et al., 2015a, 2015b). An increase in the number of seismic station deployed in the Ibero-Maghreb area (Fig. 1) occurred in the last ten years with four temporary experiments (Topolberia, Picasso, Indalo, and Siberia projects) and the densification of permanent Spanish seismic networks (Instituto Geografico Nacional and Instituto Andaluz de Geofísica). All these stations have produced a virtual seismic network with approximately ∼50–60 km of interstation spacing (Topolberia consortium, http://iberarray.ictja.csic.es). This virtual network has allowed imaging a Moho step (in some profiles a lithospheric step) that marks the approximate position of a tear fault (or STEP fault) along the northern edge of the subduction system under eastern and central Betics by receiver function migration techniques (white stars, Fig. 1, Mancilla et al., 2015a). The surface expression of this slab tearing is marked by regional uplift, denudation of high-pressure rocks in elongated core-complex type domes, late Miocene volcanism at the Eastern Betics, and by large ENE-WSW strike-slip transfer faults (see Mancilla et al., 2015a and the references therein).

The large inter-station distance, however, prevents an accurate estimation of the sharpness and size of the jump and the geometry of the contact between the subducting and the overriding plates. Trying to constrain the structure of the crust and mantle lithosphere in more details, a passive-source seismic experiment (HIRE) was conducted (Heit et al., 2010). The experiment was performed in two legs. The first leg consists of 40 broadband stations with an interstation distance of ∼2 km deployed in a NS direction perpendicular to the collision front and to the possible tear fault in central Betics (HIRE-I project, red triangles, Fig. 1). In the second leg, 10 broadband stations with an interstation distance of ∼10 km were installed to follow the lithospheric structure towards the north reaching the Iberian massif (HIRE-II project, black triangles, Fig. 1).

In this study we use the data from the HIRE high-density seismic profile and other stations in the close vicinity to perform an analysis of P-wave receiver functions in order to image with high resolution the crustal and the lithospheric mantle structures. By making use of the receiver function migration technique we delineate the Moho and lithosphere–asthenosphere boundary (LAB) and other intracrustal discontinuity across the different geological units.

2. Tectonic setting and previous geophysical studies

The westernmost Mediterranean region has undergone a complex tectonic evolution since the Miocene. In this region subduction of oceanic lithosphere beneath the tightly curved Gibraltar arc is imaged by different tomographic studies (e.g. Spakman and Wortel, 2004; Bezada et al., 2013; Villaseñor et al., 2015). The Betic and Rif orogenic belts that surround the Alboran basin conform the Gibraltar arc, the westernmost expression of the Alpine orogeny (e.g. Lonergan and White, 1997; Platt et al., 2003). These belts are formed by the westward collision of the Alboran domain and are thrusting over the South Iberian and North Maghrebian passive continental paleomargins during the Miocene (e.g. Platt et al., 2003).

In this area the Iberian and Nubian plates converge with current WNW–ESE oblique direction at a rate of ∼4–5 mm/yr (e.g. Nocquet and Calais, 2003; Stich et al., 2006; Serpelloni et al., 2007). In this convergent setting an extension process is present since Miocene times and is responsible for the development of the Alboran Basin in the middle of this collisional orogeny. The onset of this extension process is due to the evolution of the western Mediterranean subduction system toward a slab rollback system together with back-arc extension, also producing too the westward motion of the Alboran domain over the Iberian and Maghrebian paleomargins (e.g. Lonergan and White, 1997; Gutscher et al., 2002; Faccenna et al., 2004). This subduction system is currently in its last evolution stage where the subduction process seems to be no longer active (e.g. Stich et al., 2006).

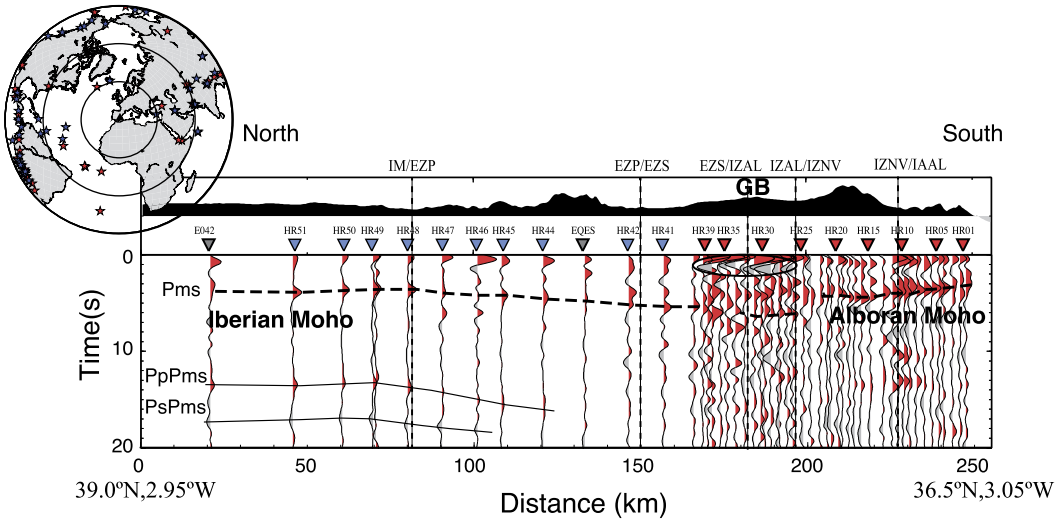

Fig. 2. Summation traces of the receiver functions for all the stations along the NS-profile shown in Fig. 1. All the traces have been corrected for Ps-moveout prior to stacking. The horizontal dashed black lines mark the converted phase at the Moho discontinuity (Pms) and the continuous black lines the arrival time of the multiples phases from the Moho. The vertical dashed lines mark the limit between different geologic units at surface (IM: Iberian massif; EZP: External Zones Prebetics; EZS: External Zones Subbetics; IZAL: Internal Zones Alpujarride; IZNV: Internal Zones Nevado-Filabride). The black circle labeled with **GB** at the top of the topography encloses the multiples related with the sedimentary cover of the Guadix Basin. The inset map shows the location of the earthquakes used in the receiver function analysis. The red stars are the ones recorded by the HIRE-I stations and blue stars by the HIRE-II stations. (For interpretation of the references to color in this figure legend, the reader is referred to the web version of this article.)

The tomographic studies, with a resolution from ∼70 km depth to the base of the mantle transition zone, reveal the current geometry of the subducted slab, imaged as a high-velocity body (e.g. Bezada et al., 2013; Palomeras et al., 2014; Villaseñor et al., 2015). This high-velocity body, possibly corresponding to oceanic lithosphere, has a slab-like structure dipping steeply towards the east. The projection of this slab on the surface has a curvilinear shape and coincides with the extension of the Gibraltar arc orogenic belts (the Betics and the Rif belts; e.g. Bezada et al., 2013).

The seismic profile analyzed in this study probes two main tectonic units of Southern Iberia involved in the collision (Fig. 1): the Betics domain sampled by the stations of HIRE-I and the Iberian Massif by the stations of HIRE-II. The Iberian massif forms a major part of the Iberian Peninsula and is a fragment of the European Variscan orogen (Fig. 1). The crustal structure in its southern part is rather homogeneous with an almost flat crust with a thickness of 30–32 km (Mancilla et al., 2015b; Mancilla and Diaz, 2015). The Betics domain is traditionally divided into the External Zones, the Internal Zones (or Alboran domain), and the Flysch units. Our experiment only samples the External and the Internal Zones units. The External Zones represent the continental paleomargin of Iberia and contain Mesozoic to Miocene sedimentary rocks deposited on this paleomargin prior to the collision and the formation of the Betics belts (Prebetic and Subbetic units, Fig. 1, Garcia-Hernandez et al., 1980). The External Zones were folded and thrusted in the northwesterly direction onto the Iberian foreland during the Miocene. The Alboran domain (or Internal Zones) is composed mainly of Paleozoic and Mesozoic meta-sedimentary rocks with varying metamorphic grade and Neogene basin deposits (Fig. 1, e.g. Lonergan and White, 1997). The Internal Zones have traditionally been divided into the Nevado-Filabride (IZNV), Alpujarride (IZAL) and Malaguide complexes (Balanyá and García-Dueñas, 1987). Only the first two complexes are observed at the surface in our study area (Fig. 1).

Mancilla et al. (2013 and 2015a, 2015b) obtained migration images of the lithospheric structure using P-wave receiver functions in NS and EW profiles along the southern Iberian Peninsula. The average inter-station distance was 50–60 km. They observed strong lateral variations of the crustal thickness with in the southern Iberia peninsula, ranging from ∼19 km to ∼46 km and a relatively thin lithosphere with thickness ranging from ∼50 km in southeastern Iberia to ∼90–100 km beneath the thickest crust and the western Betics and the Rif near the coast. The thickest crust was found at the contact between the Alboran domain and the External Zones of the Betics Range underneath some of the Neogene basins (e.g. Granada and Guadix-Baza basins). On the contrary, crustal thinning was observed in southeastern Iberia (down to 19 km). From the cross-sections, they interpreted that the Iberian crust underthrusted the Alboran domain under its contact with the External Zones and described the presence of slab-like feature of Iberian lithosphere nature at the western Betics while tearing of this Iberian slab is proposed in the central and eastern Betics regions.

3. Data and methodology

We calculate P-wave receiver functions from teleseismic seismograms recorded at 50 seismic broadband stations deployed in a North–South profile across the Sierra Nevada Mountains in central Betics, Southern Spain (red and light blue triangles, Fig. 1; HIRE project, Heit et al., 2010). The HIRE-I stations were in operation for 14 months, from 09/2010 to 11/2011, while the HIRE-II stations for 22 months, from 06/2013 to 05/2015. In addition, we use data from permanent and other temporary seismic stations located close to the profile (gray triangles, Fig. 1). The total length of the profile is ∼230 km. The additional permanent stations belong to the Instituto Andaluz de Geofísica (IAG, http://www.ugr.es/~iag) and Instituto Geográfico Nacional (IGN, http://www.ign.es) and the temporary stations were deployed by the TOPOIBERIA (Iberarray seismic network, https://doi.org/10.7914/SN/IB) and INDALO projects (http://www.ugr.es/~iag).

For the receiver function analysis, we consider earthquakes with magnitude larger than 5.5 in the distance range between 30° and 90°. The number of obtained receiver functions ranges from 8 (HR24) to 56 (HR36). The difference in the number of receiver functions between stations is mainly due to technical problems for some stations during the experiment. Additionally, we include the receiver functions from stations locate close to the profile that were analyzed by Mancilla et al. (2015b). For the study area, the azimuthal coverage of the data is shown in the inset map in Fig. 2.

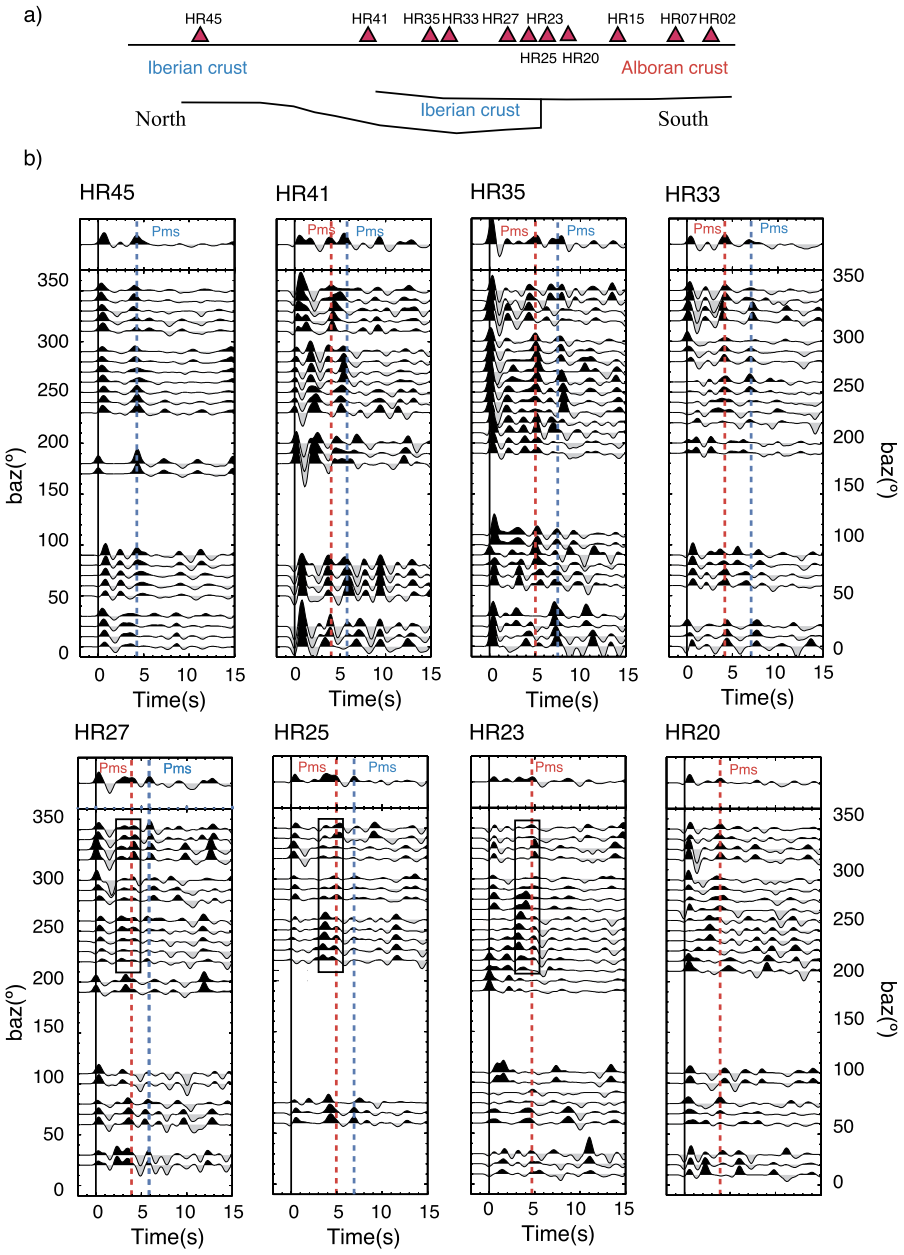

Fig. 3. a) Location of the stations shown in b) along the profile with a simplified crustal structure below them obtained in the migration image in Fig. 5; b) Q component receiver functions for some representative stations stacked by backazimuth in bins of 10° with an overlap of 5°. The summation trace of the Q components is displayed on the top. All the traces have been corrected for Ps moveout prior stacking. The dashed red and blue lines mark the arrival times for the converted phase (Pms) at the Moho discontinuity for the Alboran Moho and for the Iberian Moho, respectively. Fig. 3 continued for stations located in the southern side of the STEP fault. (For interpretation of the references to color in this figure legend, the reader is referred to the web version of this article.)

Most earthquakes occur in the active seismic areas of Central and South America while other azimuths are less represented.

P-wave receiver functions are time series containing P-to-S converted and multiples reverberated phases generated at seismic discontinuities underneath the recording stations (Vinnik, 1977; Langston, 1979). The receiver functions are obtained by deconvolving the vertical component from the horizontal components in the time window corresponding to the first P arrival and its coda. The deconvolution removes the effects of the source, the P wave propagation path, and the instrument response, retaining the information on receiver-side wave conversions caused by the local structure (Vinnik, 1977; Langston, 1979).

Prior to deconvolution, we rotate the horizontal and vertical components into the ray coordinate system, using the theoretical back azimuth and incident angles, obtaining the Q and L components instead of radial and vertical components, respectively (Vinnik, 1977). Receiver functions have been obtained using an iterative time domain deconvolution method (Ligorria and Ammon, 1999). We use a Gaussian filter width of 2.5, translating into receiver function pulses of around 1 s wide. For a more detailed description about the processing used see Mancilla et al. (2012).

We display, in Fig. 3, the Q components of the receiver functions for some representative stations along the profile located in different geologic domains. The transversal components are shown in the supplementary material (Fig. S1). We observe a great variability of receiver function between stations along the profile increasing their complexity in the contact area between the Iberian Massif and the Alboran domain (stations HR41–HR25). Even though, the transversal components contains significant energy and we observe features that can be explained by dipping

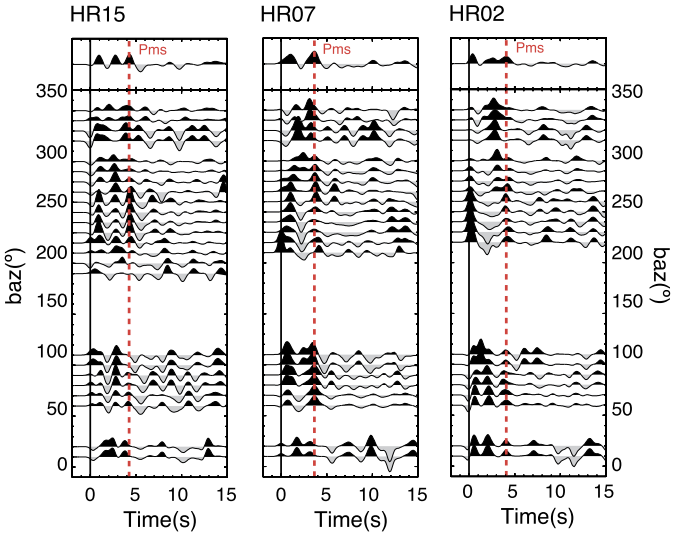

Fig. 3. (*continued*)

layers or anisotropy, in this study we only focus on the Q components. To follow the Moho discontinuity along the profile, in Fig. 2, we plot the receiver function summation traces at each station (dashed black lines).

Receiver functions show in general clear conversion phases at the Moho discontinuity (Pms) beneath most of the stations with the exception of few stations located in the Guadix-Baza basin (GB in Fig. 2 and Fig. 3). Four stations are excluded from the analysis because of the strong reverberations from the sedimentary cover that hide the conversion phase from the Moho discontinuity and other intracrustal structures. We observe strong similarities between neighboring stations (e.g. HR02 and HR07; and HR27 and HR25 in Fig. 3).

The dense distribution of HIRE-I seismic stations (red triangles Fig. 1), allows for building migration images of the lithospheric discontinuities with high spatial resolution. In Fig. 4, the PRFs are back-projected along the incident ray path and then stacked in the area with high density of stations. Data from neighboring stations within a swath of 20 km are included to build migration images. The horizontal and vertical sizes of the bins are 1 and 2 km, respectively. In the migration images we observe the continuation of the conversion discontinuities along the profile and interpret them in Fig. 4B. In the crust at the depth range of <50 km, we can identify a series of conversion phases with positive amplitudes. We interpret the deepest one (at depths of 30–50 km) as the base of the crust, and other dome-shape features as intracrustal discontinuities. A discontinuity with negative amplitude (blue color) is inferred at the depths of 60–100 km, coinciding with the LAB discontinuity observed in previous studies (Palomeras et al., 2014; Mancilla et al., 2015b). We mark the location of the inferred LAB discontinuity with magenta line.

In Fig. 5, we extend the profile toward the north with data from HIRE-I and II stations (blue line, Fig. 1) and use all the available data in the area from the closest temporary and permanent stations (gray triangles in Fig. 1). In this migration we take into account the increase of the Fresnel zone with depth. We stack in the cross-section all PRF amplitudes with piercing points inside a band with halfwidth of 20 km at both sides of the profile (Fig. 5). We spatially smooth the stacking using a Gaussian filter of 3 km. In these figures, we can delineate the Moho discontinuity and other intracrustal structures from the Iberian Massif in the north to the Mediterranean coast in the south. A modified IASP91 reference velocity model using crustal information from previous refraction profiles was used to convert delay time to depth (see Diaz and Gallart, 2009, for a review).

4. Results and discussion

The summation traces plotted in Fig. 2 along the profile in a near NS direction (dashed blue line, Fig. 1), show variations in the Pms arrival time (black-dashed lines in Fig. 2). In the southern side of the profile, receiver functions represent the response of the crustal structure underneath the Alboran domain near the Mediterranean coast. Stations HR01–HR03 show the earliest arrival of the Pms phase at ∼3 s, corresponding to a crustal thickness of ∼25 km. Towards the north, the arrival time of the Pms phase

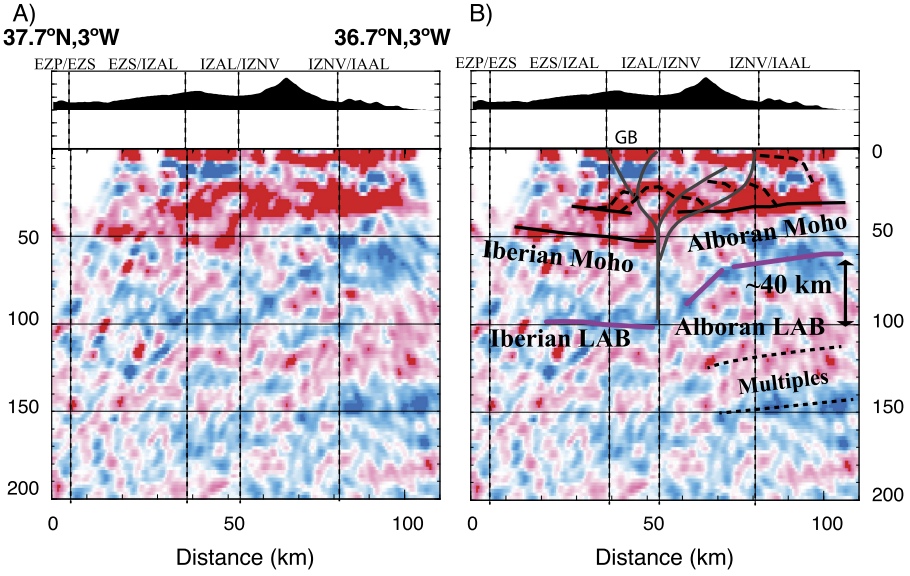

Fig. 4. A) Migration images built with receiver functions from the HIRE-I stations and neighboring stations located within a distance of 10 km from the profile at 3°W of longitude. Topography along the profile is shown at top the of each panel. In these images, positive amplitudes (red color) represent seismic discontinuities with velocity increase with depth, while negative amplitudes (blue) represent velocity decrease. B) Same as the (A) but including interpretations lines of tectonic character. Continuous black lines mark the Moho discontinuity and positives flower structure faults; the LAB discontinuity with magenta lines, and intracrustal structures with dashed black lines. We show the inferred positive flower-fault structure that propagates the tear fault toward the surface. GB marks the location of the Guadix-Baza basin. The vertical/horizontal scale is 1 to 2.

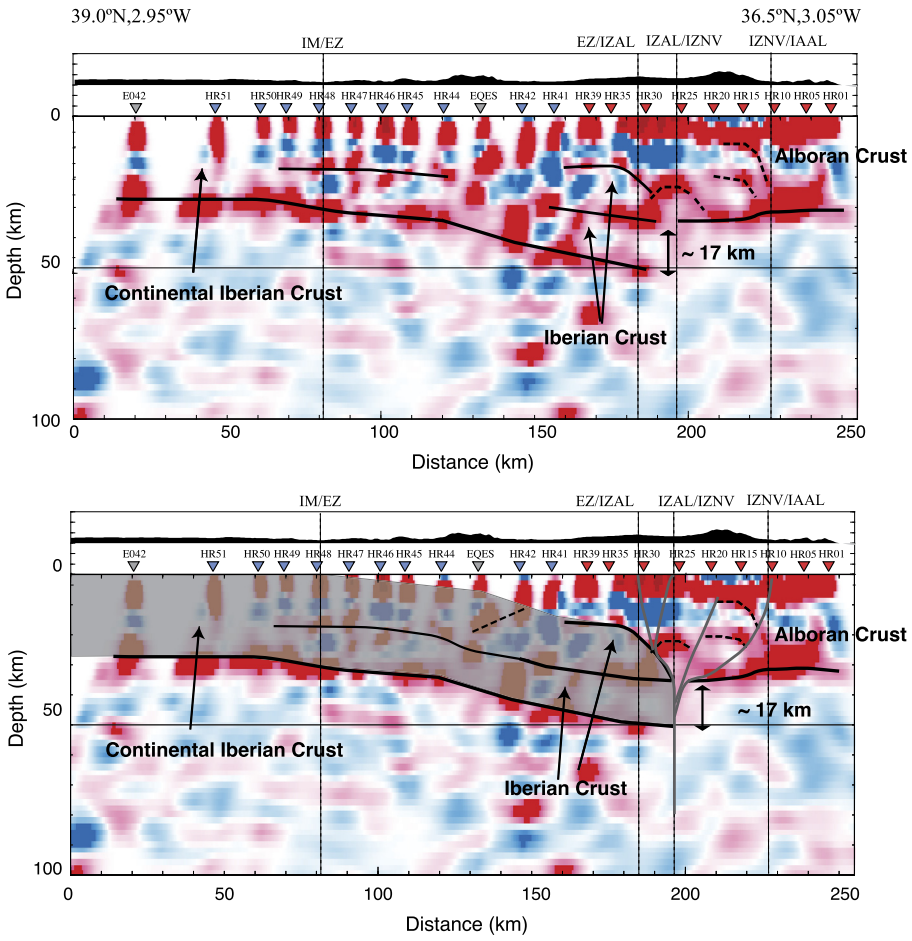

Fig. 5. Migrated P-RF along the profile marked by the dashed blue line in Fig. 1 including stations located within a half-width of 20 km at both side of the profile. The topography along the profile is displayed on the top. In the receiver function images, red color (positive amplitudes) denotes a seismic discontinuity with a velocity increase with depth. The dashed black lines mark the inferred conversion depth of the Ps converted phase at different intra-crustal discontinuities with dome-shape. With continuous lines, we delineate the bottom of the crust (black color, the Moho discontinuity) and other flat intracrustal discontinuities, and with gray color the inferred positive flower-fault structure with the vertical STEP fault (bottom panel). The transparent-gray shade marks the Iberian Massif block.

(and therefore, the crustal thickness) increases gently to ~4.5 s (~35 km) underneath stations HR17–HR18 located at the highest altitude along the profile. Farther north, the arrival time decreases to ~3.9 s (~30 km) and remains constant from station HR21 to HR24. Between stations HR25 and HR42, our data suggests the presence of two Moho phases, one pulse at approximately the same time of the Pms from the closest southern stations (~3.9 s) and the other pulse arriving later at ~5.5–7 s (implying a crustal thickness of ~46–48 km). North of station HR42, receiver functions present a simple crust and resemble the ones obtained beneath stations located in the Iberian massif (Mancilla et al., 2015b). At the northern edge of the profiles the arrival time of the Pms phases is ~3.7–3.9 (~30–32 km of crustal thickness). The arrival times and the inferred crustal thickness along the profile correlate well with results obtained by previous seismic studies and the Bouguer anomaly map (e.g. Mancilla et al., 2015b; Mancilla and Diaz, 2015).

The same pattern in crustal thickness is observed in the migration images (Figs. 4 and 5). The deepest positive conversion (continuous black line) represents the base of the crust (Moho discontinuity). The stations located in the Iberian massif present a similar crustal thickness of 30–32 km (Fig. 5). The structure of the Iberian crust remains homogeneous from the northern side of the profile until the middle of the External Zones (under station EQES, Fig. 5) where we clearly observe a stacking of crustal layers (Alboran at the top and Iberian crust at the bottom) producing an increase in the crustal thickness to a maximum of ~46–48 km.

We interpret the double phase as the stacking of the crust resulted from the continental collision where the Iberian crust underthrusts the Alboran crust (Fig. 5). The continuous increase of the crustal thickness from ~30 km under the Iberian Massif in the north to ~46–48 km underneath the External Zones (~17 km of increase) occurs within a distance of ~60 km along the profile. The crustal stacking ends very sharply below the contact at the surface between the Alpujarride and the Nevado-Filabride units (Internal zones, Figs. 4 and 5). The area with the thickest crust is below the Antiplano of the Guadix-Baza basin with an average altitude of ~1000 m but not below the highest topography along the profile (~2100 m, Sierra Nevada Mountain). This maximum crustal thickness coincides with a minimum in the Bouguer anomaly (~120–150 mGal, Bureau Gravimétrique International, http://bgi.omp.obs-mip.fr).

Towards the south, in the area where the density of seismic station increase, the observed step in the Moho discontinuity (~17 km) occurs in a short distance along the profile, less than 3 km (Fig. 4), approximately under the contact between the Nevado-Filabride and the Alpujarride units (Internal Zones). Schulte-Pelkum and Ben-Zion (2012) show that observed velocity contrasts in the crust across large continental strike-slip faults are sufficient to produce artificial vertical Moho offsets of >5 km.

From seismic refraction profile and gravity data in the area no strong velocity contrasts are found between the Iberian crust and Alboran crust (Banda et al., 1993) apart from the presence of the Guadix basin in the northern side of the STEP fault (Fig. 4). The thickness of the sedimentary cover in the influence area for our profile is less than 1000 m in its thickest part (Sanz de Galdeano et al., 2007). Even though this contrast could bias the size of the Moho step, the error is less than 4 km (Schulte-Pelkum and Ben-Zion, 2012).

This step at crustal level correlates with a step of ∼40 km at lithospheric level (magenta lines at the bottom panels in Fig. 4). In Fig. 4, we can observe a negative converted phase below the Moho at a depth of ∼100 km in the north (at distance of 20–50 km), which shallows to a depth of ∼60 km until the southern end of the profile (at distance of 100 km). We interpret this negative phase as the LAB. In general, the conversion phase at the LAB, for average lithospheric thickness, is difficult to detect in P-wave receiver functions analysis because it is often interfered by crustal multiples. In our case, the crustal multiples arrive later than the LAB phase arrival, which enables the identification of the LAB discontinuity (Fig. 4). Following the profile from north to south the LAB depth increases from 85–90 km to 100 km depth underneath the Moho discontinuity jump and suddenly decreases to ∼60 km in the south (Fig. 4). Similar values are obtained in previous studies in the area using P-wave receiver functions (Mancilla et al., 2015b), S receiver functions (Dundar et al., 2011; Heit et al., 2017) and surface wave tomography (Palomeras et al., 2014, 2017).

The anomalies in the crust and mantle lithosphere are vertically correlated (Fig. 4). The STEP fault is almost vertical from the LAB discontinuity (at ∼100 km depth) through the Moho discontinuity (at 48 km depth in the northern side) until reaching ∼30 km depth. The vertical aspect is inferred by the observed Moho step with a jump of ∼17 km between stations separated less than 5 km (between stations HR27 and HR25, Fig. 3). The spacing between stations (∼2 km) allows mapping with high accuracy the variations of the crustal structure in short distance. Therefore, the lithospheric mantle and the underthrusting Iberian crust are cut almost vertically. Above the lithospheric step, from 30 km depth to the surface, we observe at the top of the step and mostly at its left side intra-crustal structures with dome shapes (marked by dashed lines in Figs. 4 and 5) that resemble positive flower structures observed in seismic reflection profiles. We draw the possible segments of the flower structure along the changes in the continuation of the discontinuities and we connect them to the geologic boundaries at the surface.

Positive flower structures are present in transpressional settings (e.g., Park, 1993; Kearey et al., 2009) such as the central Betics region (e.g., Sanz de Galdeano et al., 1985). In central Betics the compression component came from the oblique collision between Iberia and Nubia in a current WNW-ESE direction (e.g., Nocquet and Calais, 2003; Stich et al., 2006; Serpelloni et al., 2007). The transcurrent movement needed to produce the positive flower structure came from the rollback process directed toward the west (e.g., Lonergan and White, 1997).

The inferred positive flower structure seems to extend for 60 km along the profile and 30 km in the vertical direction cutting mainly the Alboran crust. The presumed fault segments of the positive flower fault structure correlate well, in its southern part, with the observed faults of the Alpujarran Corridor (Sanz de Galdeano et al., 1985). In the northern part, the surface expressions of the flower structure are included in a narrow deformation zone between the External (Iberian paleomargin units) and Internal Zones (Alboran Domain) of the Betic Cordillera (e.g. Smet, 1984; Sanz de Galdeano et al., 1985) (Figs. 4 and 5). This ENE-SSW zone is characterized by sub-vertical faults, with an important right-lateral component of movement, separating pluri-kilometer lense-shape domains belonging to the Iberian paleomargin units or Alpujarride units (Alboran Domain). This strike-slip deformation zone, also called External Internal Shear Zone (EISZ), is the southwestern spatial continuation of the Crevillente fault (e.g., Sanz de Galdeano et al., 1985; Nieto and Rey, 2004), and can be mapped to the northern boundary of Sierra Harana where transpressive structures have been classically defined (e.g. Sanz de Galdeano et al., 1985). Thus, the outcrop of the Nevado-Filabride complex in the Sierra Nevada mountains would be the central part of this flower structure bounded by these two major right-lateral strike-slip shear bands (Alpujarran Corridor to the south and EISZ to the north). This strike-slip fault system started developing in the Middle Miocene and presents remarkable tectonic deformation and uplifting since the Late Miocene (e.g., Sanz de Galdeano et al., 1985; Martínez-Martínez et al., 2006). The dextral strike–slip Socovos Fault in the central Betics may represent one of the surface expressions of this process. The $^{40}Ar/^{39}Ar$ analysis of the lamproites melts channelized along the Socovos Fault shows an age of 9.3–7.1 Ma, which are compatible with a right-lateral lithosphere tearing in the Miocene (Pérez-Varela et al., 2013).

STEP faults can be expressed by shear zones in the crust and mantle lithosphere, associated to the tearing process at depth. However, it is not clear, how the strain and deformation are distributed in the overriding plate and if there is regional difference in the sharpness of the shear zone. Large shear zones at the surface of the overriding plate associated with STEP faults have been observed in other regions with average width in the order of 40–60 km: e.g. The Pliny-Strabo shear zone (Özbakır et al., 2013); and the Ionian fault system in the Messina Strait, (e.g. Bianchi et al., 2016). The width is similar to one we observe in this study. Özbakır et al. (2013) argue that such a width is because its immaturity evolving towards a more localized strain onto a most localize single fault. However, the sharp crustal step observed here and the tectonic flower structure observed implies a more localized shear strain distribution at crustal level, that marks the termination of the underthrusting of the Iberian Massif crust beneath the Alboran crust.

In the collision between the Iberian and Alboran domains the highest deformation is found in the Alboran crust. In contrast, the Iberian crust maintains its structure unperturbed, as suggested by the continuity in its internal structure until the collisional front. The dome structures observed by field works in Sierra Nevada, Sierra de los Filabres and Sierra Alhamilla Mountains in the Internal Zones were proposed to be crustal-scale feature (e.g., Martínez-Martínez et al., 2002). In Fig. 4, similar dome structures have been imaged in the Alboran crust (Internal Zones) confirming that hypothesis. The lateral extension of shallowest one is coincident with the Nevado-Filabride outcrop in that part of the Sierra Nevada Mountains (Martínez-Martínez et al., 2002).

Our interpretation is that a lithospheric step was produced by a STEP fault that disconnects the transitional crust of the Iberian paleomargin from the oceanic slab imaged under the Alboran Sea. This fault represents the lateral removal of the underthrusted Iberian lithosphere along the northern edge of the westernmost Mediterranean subduction system. The tearing of the Iberian lithosphere along this fault presumably occurred as a consequence of the reduction in the roll-back velocity at the northern edge of the subduction system when the southern Iberian continental margin started to be subducted, compared with the roll-back velocity below the Alboran basin where oceanic lithosphere were consuming (e.g. Duggen et al., 2004, 2005). The expected consequence of this change in velocity along the strike of the subduction system is the tear of the oceanic lithosphere from the continental-transitional lithosphere along sub-vertical tear faults called STEP fault (Govers and Wortel, 2005). This type of fault is present or thought to be

present at the edges of many subduction systems as Calabria and Hellenic arc in the Mediterranean Sea (e.g. Gallais et al., 2013; Govers and Wortel, 2005).

In general, the STEP faults develop, mainly, along continent–oceanic boundaries of the same lithospheric plate, e.g., along South the American-Caribbean plate boundary, in the Calabria arc, in western Algeria margin (Clark et al., 2008; Gallais et al., 2013; Badji et al., 2015), but sometimes in purely oceanic domains, e.g., in South Sandwich trench and Tonga subduction zone (Govers and Wortel, 2005). However, we observe that in central Betics, the tearing seems to occur at the transitional lithosphere instead of at the boundary between the continental–oceanic lithosphere as expected (Govers and Wortel, 2005). The thickness of the removed underthrusted Iberian crust is ∼17–20 km (Fig. 5). The structure of the Iberian crust remains constant from the northern side of the profile until the contact with the External Zone. This continuity and the thickness of the removed Iberian crust imply a transitional character. That could mean that tearing of this transitional lithosphere probably occurred along inherited weaknesses of the pre-rifted continental paleomargin (García-Hernandez et al., 1980).

In the central Betics, the surface expression of the inferred STEP fault is marked by regional uplift, denudation of high-pressure rocks in elongated core-complex type domes (e.g., Sierra Nevada Mountains), late Miocene volcanism at Eastern Betics, and by large ENE–WSW strike-slip transfer faults (e.g. Platt et al., 2006, 2013).

Another important result from the migration images is the absence of correlation among the highest altitude along the profile and the biggest crustal and lithospheric thicknesses (Figs. 4 and 5). The coincidence of the highest topography with the positive flower structure suggests that at least part of this topography is produced by this compressive structure. However, this structure could not be enough to explain a mean uplift of 0.5 mm/y during last 8 Ma (Azañón et al., 2015). The lithospheric removal should promote a complementary asthenospheric push up to this area. In western Betics, Heit et al. (2017) found that the highest topography of Sierra Nevada Mountain correlates well with a possible asthenospheric influx due to ongoing delamination, at the position where they detected a jump in the depth of the LAB discontinuity.

5. Conclusions

We image, by migrating P receiver functions, the crustal and lithospheric architecture in the high-metamorphic core of the central Betic orogen and its transition to the Variscan terrains of the Iberian Massif in the north. We observe that the underthrusted Iberian lithosphere terminates sharply under the contact at the surface between the Alpujarride and the Nevado-Filabre complexes (Alboran domain). The abrupt ending of the underthrusted Iberian lithosphere produces a sharp Moho and lithospheric step of ∼17 km and 40 km, respectively. This sharp and prominent lithospheric step is related with a near-vertical STEP fault that propagates to the surface as a positive flower fault structure. This STEP fault accommodated the differences in the subduction rollback velocity along the strike, at the northern edge of the Western Mediterranean system, when the Iberian continental lithosphere started subducting under the Alboran domain. We have not observed a crustal root under the highest altitude of the Sierra Nevada mountain, suggesting that the high topography is produced by the combination of the uplift produced by the positive flower structure and the push up of the asthenosphere after the lithospheric removal of the underthrusting Iberia along the STEP fault.

Acknowledgements

We are grateful to the staff involved in HIRE and TRANSCORBE projects for their hard work in the acquisition of field data and in the permanent networks (IGN and IAG). The Geophysical Instrument Pool of Potsdam provided seismic equipment for the HIRE and TRANSCORBE experiments. We are grateful, too, to Rainer Kind and Christian Haberland for their support. We acknowledge the comments and suggestions made by Rob Govers and an anonymous reviewer that improve the paper. This work was supported by the projects: CGL2015-67130-C2-2-R, GCL2012-31472 (TRANSCORBE), HIRE (GFZ Potsdam) and PP2012-PIJD003 (Granada University). We acknowledge work on free softwares SAC and GMT.

Appendix A. Supplementary material

Supplementary material related to this article can be found online at https://doi.org/10.1016/j.epsl.2018.01.008.

References

Agostinetti, N.P., 2015. The structure of the Moho in the Northern Apennines: evidence for an incipient slab tear fault? Tectonophysics 655, 88–96.

Azañón, J.M., Galve, J.P., Pérez-Peña, J.V., Giaconia, F., Carvajal, R., Booth-Rea, G., Jabaloy, A., Vázquez, M., Azor, A., Roldán, F.J., 2015. Relief and drainage evolution during the exhumation of the Sierra Nevada (SE Spain): is denudation keeping pace with uplift? Tectonophysics 663, 19–32.

Badji, R., Charvis, P., Bracene, R., Galve, A., Badsi, M., Ribodetti, A., Benaissa, Z., Klingelhoefer, F., Medaouri, M., Beslier, M-O., 2015. Geophysical evidence for a transform margin offshore Western Algeria: a witness of a subduction-transform edge propagator? Geophys. J. Int. 200 (2), 1029–1045. https://doi.org/10.1093/gji/ggu454.

Baes, M., Govers, R., Wortel, R., 2011. Subduction initiation along the inherited weakness zone at the edge of a slab: insights from numerical models. Geophys. J. Int. 184, 991–1008. https://doi.org/10.1111/j.1365-246X.2010.04896.x.

Balanyá, J.C., García-Dueñas, V., 1987. Les directions structurales dans le Domaine d'Alborán de part et d'autre du Détroit de Gibraltar. C. R. Acad. Sci. Paris, Ser. II 304, 929–932.

Banda, E., Gallart, J., Garcia-Dueñas, V., Dañobeitia, J.J., Makris, J., 1993. Lateral variation of the crust in the Iberia Peninsula: new evidence from the Betic Cordillera. Tectonophysics 221, 53–66.

Bezada, M.J., Hymphreys, E.D., Toomey, D.R., Harnafi, M., Dávila, J.M., Gallart, J., 2013. Evidence for slab rollback in westernmost Mediterranean from improved upper mantle imaging. Earth Planet. Sci. Lett. 368, 51–60.

Bianchi, I., Lucente, F.P., Di Bona, M., Govoni, A., Agostinetti, N.P., 2016. Crustal structure and deformation across a mature slab tear zone: the case of southern Tyrrhenian subduction (Italy). Geophys. Res. Lett. 43, 12380–12388. https://doi.org/10.1002/2016GL070978.

Clark, S.A., Zelt, C.A., Magnani, M.B., Levander, A., 2008. Characterizing the Caribbean–South American plate boundary at 64°W using wide-angle seismic data. J. Geophys. Res. 113, B07401. https://doi.org/10.1029/2007JB005329.

De Smet, M.E.M., 1984. Wrenching in the external zone of the Betic Cordilleras southern Spain. Tectonophysics 107 (1–2), 57–79.

Díaz, J., Gallart, J., 2009. Crustal structure beneath the Iberian Peninsula and surrounding waters: a new compilation of deep seismic sounding results. Phys. Earth Planet. Inter. 173, 181–190. https://doi.org/10.1016/j.pepi.2008.11.008.

Duggen, S., Hoernle, K., van der Bogaard, H., 2004. Magmatic evolution of the Alboran region: the role of subduction in forming the western Mediterranean and Messian salinity crisis. Earth Planet. Sci. Lett. 218, 91–108.

Duggen, S., Hoernle, K., van den Bogaard, P., Garbe-Schonberg, D., 2005. Post-collisional transition from subduction- to intraplate-type magmatism in the westernmost Mediterranean: evidence for continental-edge delamination of subcontinental Lithosphere. J. Petrol. 46, 1155–1201.

Dundar, S., et al., 2011. Receiver function images of the base of the lithosphere in the Alboran Sea region. Geophys. J. Int. 187, 1019–1026.

Faccenna, C., Piromallo, C., Crespo-Blanc, A., Jolivet, L., Rossetti, F., 2004. Lateral slab deformation and the origin of the western Mediterranean arcs. Tectonics 23, TC1012. https://doi.org/10.1029/2002TC001488.

Gallais, F., Graindorgeb, D., Gutscher, M.-A., Klaeschend, D., 2013. Propagation of a lithospheric tear fault (STEP) through the western boundary of the Calabrian accretionary wedge offshore eastern Sicily (Southern Italy). Tectonophysics 602, 141–152. https://doi.org/10.1016/j.tecto.2012.12.026.

García-Castellanos, D., Villaseñor, A., 2011. Messian salinity crisis regulated by competing tectonics and erosion at the Gibraltar Arc. Nature 480, 359–363.

García-Hernández, M., López-Garrido, A., Rivas, P., Sanz de Galdeano, C., Vera, J., 1980. Mesozoic paleogeographic evolution of the External Zones of the Betics Cordillera. Geol. Mijnb. 59, 155–176.

Govers, R., Wortel, M.J.R., 2005. Lithosphere tearing at STEP faults: response to edges of subduction zones. Earth Planet. Sci. Lett. 236, 505–523.

Gutscher, M.-A., Malod, J., Rehault, J.-P., Contrucci, I., Klingelhoefer, F., Mendes-Victor, L., Spakman, W., 2002. Evidence for active subduction beneath Gibraltar. Geology 30 (12), 1071–1074. https://doi.org/10.1130/0091.

Heit, B., Yuan, X., Mancilla, F., 2010. High resolution seismological profiling across Sierra Nevada (HIRE), Deutsches GeoForschungsZentrum GFZ. Other/Seismic Network. https://doi.org/10.14470/4P7565788335.

Heit, B., Mancilla, F.d.L., Yuan, X., Morales, J., Stich, D., Martín, R., Molina-Aguilera, A., 2017. Tearing of the mantle lithosphere along the intermediate-depth seismicity zone beneath the Gibraltar Arc: the onset of lithospheric delamination. Geophys. Res. Lett. 44, 4027–4035. https://doi.org/10.1002/2017GL073358.

Kearey, P., Klepeis, K.A., Vine, F.J., 2009. Global Tectonics, 3rd ed. Wiley-Blackwell, Oxford. 482 p.

Langston, C.A., 1979. Structure under Mount Rainier, Washington, inferred from teleseismic body waves. J. Geophys. Res. 84, 4749–4762.

Ligorria, J.P., Ammon, C.J., 1999. Iterative deconvolution and receiver function estimation. Bull. Seismol. Soc. Am. 89, 1395–1400.

Lonergan, L., White, N., 1997. Origin of the Betic-Rif mountain belt. Tectonics 16, 504–522.

Nieto, L.M., Rey, J., 2004. Magnitude of lateral displacement on the Crevillente Fault Zone (Betic Cordillera, SE Spain): stratigraphical and sedimentological considerations. Geol. J. 39 (1), 95–110.

Nijholt, N., Govers, R., 2015. The role of passive margins on the evolution of Subduction-Transform Edge Propagators (STEPs). J. Geophys. Res., Solid Earth 120, 7203–7230. https://doi.org/10.1002/2015JB012202.

Mancilla, F., Stich, D., Morales, J., Julià, J., Diaz, J., Pazos, A., Córdoba, D., Pulgar, J.A., Ibarra, P., Harnafi, M., Gonzalez-Lodeiro, F., 2012. Crustal thickness variations in northern Morocco. J. Geophys. Res. 117, B02312. https://doi.org/10.1029/2011JB008608.

Mancilla, F., Booth-Rea, G., Stich, D., Pérez-Peña, J.V., Morales, J., Azañon, J.M., Martin, R., Giacomia, F., 2015a. Slab rupture and delamination under the Betics and Rif constrained from receiver functions. Tectonophysics 663, 225–237. https://doi.org/10.1016/j.tecto.2015.06.028.

Mancilla, F., Stich, D., Morales, J., Martin, R., Diaz, J., Pazos, A., Cordoba, D., Pulgar, J.A., Ibarra, P., Harnafi, M., Gonzalez-Lodeiro, F., 2015b. Crustal Thickness and Images of the Lithospheric discontinuities in the Gibraltar arc and surrounding areas. Geophys. J. Int. 203 (3), 1804–1820. https://doi.org/10.1093/gji/ggv390.

Mancilla, F., Diaz, J., 2015. High resolution Moho topography map beneath Iberia and Northern Morocco from receiver function analysis. Tectonophysics 663, 203–211. https://doi.org/10.1016/j.tecto.2015.06.017.

Martínez-Martínez, J.M., Soto, J.I., Balanyá, J.C., 2002. Orthogonal folding of extensional detachments: structure and origin of the Sierra Nevada elongated dome (Betics, SE Spain). Tectonics 21 (3), 1012. https://doi.org/10.1029/2001TC001283.

Martínez-Martínez, J.M., Booth-Rea, G., Azañón, J.M., Torcal, F., 2006. Active transfer fault zone linking a segmented extensional system (Betics, southern Spain): insight into heterogeneous extension driven by edge delamination. Tectonophysics 422 (1), 159–173. https://doi.org/10.1016/j.tecto.2006.06.001.

Nocquet, J.M., Calais, E., 2003. Crustal velocity field of western Europe from permanent GPS array solutions, 1996–2001. Geophys. J. Int. 154, 72–88.

Özbakır, A.D., Şengör, A.M.C., Wortel, M.J.R., Govers, R., 2013. The Pliny–Strabo trench region: a large shear zone resulting from slab tearing. Earth Planet. Sci. Lett. 375. https://doi.org/10.1016/j.epsl.2013.05.025.

Palomeras, I., Thurner, S., Levander, A., Liu, K., Villasenor, A., Carbonell, R., Harnafi, M., 2014. Finite-frequency Rayleigh wave tomography of the western Mediterranean: mapping its lithospheric structure. Geochem. Geophys. Geosyst. 15, 140–160. https://doi.org/10.1002/2013GC004861.

Palomeras, I., Villaseñor, A., Thurner, S., Levander, A., Gallart, J., Harnafi, M., 2017. Lithospheric structure of Iberia and Morocco using finite-frequency Rayleigh wave tomography from earthquakes and seismic ambient noise. Geochem. Geophys. Geosyst. 18. https://doi.org/10.1002/2016GC006657.

Pearce, F.D., Rondenay, S., Sachpazi, M., Charalampakis, M., Royden, L.H., 2012. Seismic investigation of the transition from continental to oceanic subduction along the western Hellenic Subduction Zone. J. Geophys. Res. 117, B07306. https://doi.org/10.1029/2011JB009023.

Park, R.G., 1993. Geological Structures and Moving Plates, 2nd ed. Chapman & Hall, Glasgow. 337 p.

Pérez-Valera, L.A., Rosenbaum, G., Sánchez-Gómez, M., Azor, A., Fernández-Soler, J.M., Pérez-Valera, F., Vasconcelos, P.M., 2013. Age distribution of lamproites along the Socovos Fault (southern Spain) and lithospheric scale tearing. Lithos 180–181, 252–263.

Platt, J.P., Allerton, S., Kirker, A., Mandeville, C., Mayfield, A., Platzman, E.S., Rimi, A., 2003. The ultimated arc: differential displacement, oroclinal bending, and vertical axis rotation in the external Betic-Rif arc. Tectonics 22 (3), 1017. https://doi.org/10.1029/2001TC001321.

Platt, J.P., Anczkiewicz, R., Soto, J.I., Kelley, S.P., Thirlwall, M., 2006. Early Miocene continental subduction and rapid exhumation in the western Mediterranean. Geology 34, 981–984.

Platt, J.P., Beher, W.M., Johanesen, K., Williams, J.R., 2013. The Betic-Rif arc and its orogenic hinterland: a review. Annu. Rev. Earth Planet. Sci. 41, 313–357.

Sanz de Galdeano, C., Rodriguez-Fernandez, J., López-Garrido, A.C., 1985. A strike-slip fault corridor within the Alpujarra mountains (Betic Cordilleras, Spain). Geol. Rundsch. 74 (3), 641–655. https://doi.org/10.1007/bf01821218.

Sanz de Galdeano, C., Delgado, J., Galindo-Zaldívar, J., Marín-Lechado, C., Alfaro, P., García Tortosa, F.J., López-Garrido, A.C., Gil, A.J., 2007. Anomalías gravimétricas de la cuenca de Guadix-Baza (Cordillera Bética, España). Bol. Geol. Min. 118 (4), 763–774.

Serpelloni, E., Vannucci, G., Pondrelli, S., Argnani, A., Casula, G., Anzidei, M., Baldi, P., Gasperini, P., 2007. Kinematics of the western Africa–Eurasia plate boundary from focal mechanisms and GPS data. Geophys. J. Int. 169, 1180–1200. https://doi.org/10.1111/j.1365-246X.2007.03367.x.

Schulte-Pelkum, Vera, Ben-Zion, Yehuda, 2012. Apparent vertical Moho offsets under continental strike-slip faults from lithology contrasts in the seismogenic crust. Bull. Seismol. Soc. Am. 102 (6), 2757–2763. https://doi.org/10.1785/0120120139.

Spakman, W., Wortel, R., 2004. A tomographic view on Western Mediterranean geodynamics. In: Cavazza, W., Roure, F.M., Spakman, W., Stampfli, G.M., Ziegler, P.A. (Eds.), The Transmed Atlas, the Mediterranean Region from Crust to Mantle. Springer, Berlin–Heidelberg, pp. 31–52.

Stich, D., Serpelloni, E., de Lis Mancilla, F., Morales, J., 2006. Kinematics of the Iberia-Maghreb plate contact from seismic moment tensors and GPS observations. Tectonophysics 426, 295–317.

Villaseñor, A., Chevrot, S., Harnafi, M., Gallart, G., Pazos, A., Serrano, I., Córdoba, D., Pulgar, J.A., Ibarra, P., 2015. Subduction and volcanism in the Iberia–North Africa collision zone from tomographic images of the upper mantle. Tectonophysics 663, 238–249. https://doi.org/10.1016/j.tecto.2015.08.042.

Vinnik, L.P., 1977. Detection of waves converted from P to SV in the mantle. Phys. Earth Planet. Inter. 15, 39–45.